# A New Insight into the Mechanism of the Tabletability Flip Phenomenon

Zijian Wang<sup>1</sup>, Chenguang Wang<sup>1</sup>, Yiwang Guo<sup>1</sup>, Deepak Bahl<sup>2</sup>, Alex Fok<sup>3</sup>, Changquan Calvin Sun<sup>1,\*</sup>

<sup>1</sup> Pharmaceutical Materials Science and Engineering Laboratory, Department of Pharmaceutics, College of Pharmacy, University of Minnesota, USA

<sup>2</sup> Bristol-Myers Squibb, 556 Morris Avenue, Summit, NJ 07901, USA

<sup>3</sup> Minnesota Dental Research Center for Biomaterials and Biomechanics, School of Dentistry, University of Minnesota, USA

\* Corresponding author

Changquan Calvin Sun, Ph.D.

9-127B Weaver-Densford Hall

308 Harvard street S.E.

Minneapolis, MN 55455

Email: sunx0053@umn.edu

Tel: +1-612-624-3722

Fax: +1-612-626-2125

#### Abstracts

1

Tabletability is an outcome of interparticulate bonding area (BA) – bonding strength (BS) interplay, 2 influenced by the mechanical properties, size and shape, surface energetics of the constituent 3 particles, and compaction pressure. Typically, a more plastic active pharmaceutical ingredient 4 (API) exhibits a better tabletability than less plastic APIs due to the formation of a larger BA 5 during tablet compression. Thus, solid forms of an API with greater plasticity are traditionally 6 7 preferred if other critical pharmaceutical properties are comparable. However, the tabletability flip phenomenon (TFP) suggests that a solid form of an API with poorer tabletability may exhibit 8 9 better tabletability when formulated with excipients. In this study, we propose another possible mechanism of TFP, wherein softer excipient particles conform to the shape of harder API particles 10 during compaction, leading to a larger BA under certain pressures and, hence, better tabletability. 11 In this scenario, the BA-BS interplay is dominated by BA. Accordingly, TFP should tend to occur 12 when API solid forms are formulated with a soft excipient. We tested this hypothesis by visualizing 13 the deformation of particles in a model compressed tablet by nondestructive micro-computed 14 tomography and by optical microscopy when the particles were separated from the tablet. The 15 results confirmed that soft particles wrapped around hard particles at their interfaces, while an 16 17 approximately flat contact was formed between two adjacent soft particles. In addition to the direct visual evidence, the BA-dominating mechanism was also supported by the observation that TFP 18 occurred in the p-aminobenzoic acid polymorph system only when mixed with a soft excipient. 19

20

21

- **Key words:** tabletability, tabletability flip, bonding area, bonding strength, plasticity, mixtures,
- 22 particle deformation

## 1. Introduction

23

24

25

26

27

28

29

30

31

32

33

34

35

36

37

38

39

40

41

42

43

44

45

46

47

48

49

50

51

52

53

The oral tablet is a preferred pharmaceutical dosage form for drug delivery due to its excellent physical and chemical stability, ease of administration, precise dosing, customized dissolution performance, high manufacturing efficiency and low manufacturing cost (Nyol and Gupta, 2013; Rudnic, 2002; Ubhe and Gedam, 2020). For a tablet product to be successful, it must possess adequate mechanical strength to remain intact post manufacturing until administration by consumers. This necessitates sufficient tabletability - the ability of a powder to form a tablet of specific strength under the effect of compaction pressure (Sun and Grant, 2001).

Tabletability is determined by the interplay between bonding area (BA) and bonding strength (BS) between the particles, with the former influenced by their mechanical properties, particulate properties, and compaction conditions, and the latter influenced by the nature of the materials (Sun, 2011). For examples, plastic deformation of ductile powders during die compression also explains the strength anisotropy (stronger along the radial direction than the compaction direction) (Galen and Zavaliangos, 2005). Successful simulation of plastically deforming powder compaction requires accurate mechanical properties as input parameters (Cocks and Sinka, 2007). Particle size can affect, sometimes significantly, tabletability of materials (Mckenna and Mccafferty, 1982; Paul et al., 2019). It is also well known that tableting performance is also affected by the process parameters employed during tablet manufacturing (Sinka et al., 2009). Typically, a more plastic active pharmaceutical ingredient (API) can undergo more extensive plastic deformation under compression, resulting in a larger BA and better tabletability (Chang and Sun, 2017; Chen et al., 2022; Hu et al., 2019). Therefore, a more plastic solid form of an API is generally preferred for formulation development due to its enhanced tabletability. However, the occurrence of the tabletability flip phenomenon (TFP), where a less plastic API with poorer tabletability can exhibit better tabletability when formulated in the same excipient matrix (Paul et al., 2020; Wang et al., 2023), calls for caution in such preferences. Previous studies have indicated that TFP tends to manifest when the compaction pressure is high or when there is a significant difference in plasticity between two solid forms (Wang et al., 2023). Understanding the mechanism of TFP is critical for predicting the compaction properties of mixtures, providing invaluable insights for efficient and reliable tablet formulation design.

A previously proposed mechanism suggests that TFP results from a shift in the dominating factor in the BA-BS interplay from BA to BS upon formulation (Paul et al., 2020). In other words,

the previous mechanism assumes that BAs of mixtures do not differ significantly when two APIs are mixed with a more plastic excipient. Consequently, the tabletability of a mixture is higher for the less plastic API, which exhibits a higher BS. This mechanism holds true only if the excipient is significantly softer than both API forms, satisfying the assumption of comparable BA in the tablets of the two mixtures. However, this condition was not always satisfied in the previous cases of TFP. Hence, a different mechanism is required to explain the TFP when the plasticity of the excipient is not significantly higher than both API solid forms. A correct mechanistic understanding of the TFP is essential for developing effective strategies to either overcome the TFP or guide the design of tablet formulation for better tabletability (Sun, 2009). Accordingly, we carried out this work to explore an alternative mechanism of TFP.

## 2. BA dominating mechanism

When only one type of constituent particles is present, the ease of deformation is the same for two adjacent particles during compression. Consequently, a flat contact area is formed between adjacent particles. In this case, the BA for a less plastic material is smaller (Figure 1a, b). It follows that, under identical compaction conditions, a softer API undergoes more extensive plastic deformation, leading to a larger BA and better tabletability. In contrast, an intact tablet may not be obtained for very hard particles if the compaction pressure does not induce a significant degree of plastic deformation, resulting in a negligible BA. The situation changes when the contact involves two particles with different plasticity. In such cases, the contact area is not flat, and the more extensive plastic deformation of the softer particle results in its "wrapping" around the harder particle. This scenario is consistent with observations made in some other studies. It was shown that the lead (soft)-Al<sub>2</sub>O<sub>3</sub> (hard) tablets obtained by cyclic pressing had higher strength than those made by static pressing (Zavaliangos and Laptev, 2000). This was because that soft lead can further deform during repeated compaction steps to fill up more void in the tablet, resulting in larger BA and higher tablet density. Moreover, lead-lead and lead-alumina contacts deform easier and contribute to densification more than the contact of alumina-alumina. For accurate numerical simulation of compaction behaviors of solid mixtures with very different mechanical properties (rigid vs. soft), it is also important to recognize that the development of contact area between two particles during compaction is dominated by the softer particle (Li et al., 2009).

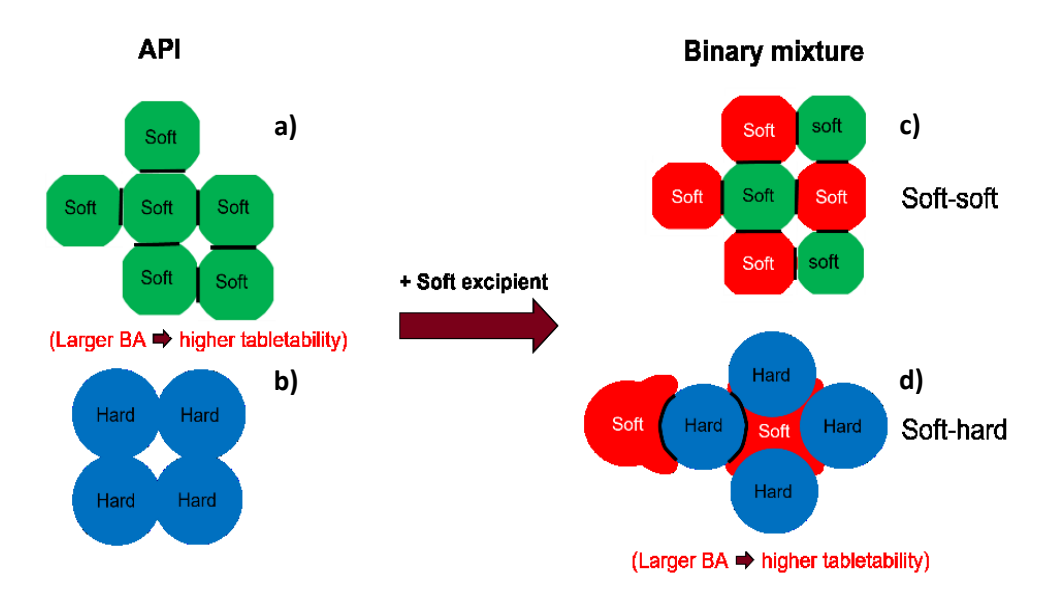


Figure 1. The bonding area-dominating mechanism for the tabletability flip phenomenon.

In the case of a mixture comprising a soft API and a soft excipient, a flat contact between adjacent particles is expected during compaction, similar to that between two soft API particles (Figure 1a, c). On the other hand, in a mixture of a soft excipient and a hard API, the soft excipient particles will undergo more plastic deformation than the hard API particles during compaction. This could result in a contact zone where the soft particle conforms to the shape of the hard API particle (Figure 1d). This phenomenon is analogous to a hard tip penetrating into a soft surface during an indentation experiment, leading to a larger BA than that between soft and soft particles. As a consequence, while the harder API by itself exhibits poorer tabletability than the softer API due to a smaller BA (Figure 1b), the presence of a soft excipient can result in a mixture with better tabletability for the harder API than for the softer API, thus demonstrating the tabletability flip phenomenon. Importantly, this mechanism predicts an absence of TFP when a hard excipient is mixed with the same two APIs, assuming that there are no significant differences in the BS or other pertinent properties between corresponding systems. This is because a harder API would still result in a smaller BA in such a mixture than a softer API.

To validate the described mechanism, we conducted a direct examination of the differential particle deformation behaviors responsible for the TFP on a model tablet using micro-computed tomography (micro-CT) and optical microscopy. The mechanism was further confirmed by successfully producing TFP between two *p*-aminobenzoic acid (ABA) polymorphs in the presence

of a soft excipient, microcrystalline cellulose (MCC), as well as showing the absence of TFP when a hard excipient, calcium hydrogen phosphate dihydrate (DCPD), was used.

#### 3. Materials and methods

#### 3.1 Materials

PlayDoh (Hasbro, Pawtucket, RI, USA), glass beads with a diameter of 1 mm (Thermo Fisher Scientific, Fair Lawn, NJ, USA), magnesium stearate (MgSt; Covidien; Dublin, Ireland), p-Aminobenzoic acid α form (ABAα, Thermo Scientific Chemicals, Waltham, MA, USA), Microcrystalline cellulose (MCC; Avicel PH105, FMC; Newark, DE, USA), Calcium Hydrogen Phosphate Dihydrate (DCPD, Emcompress®, JRS Pharma; Patterson, NY, USA), and Methanol (Sigma-Aldrich; St. Louis, MO, USA) were purchased from respective vendors and used as received. Round PlayDoh particles (1 - 2 mm diameter) were prepared manually by rolling. The sizes of the PlayDoh particles and glass beads were chosen so that the micro-CT images of the model tablet had sufficient spatial resolution for delineating the contact area between neighboring particles.

## 3.2 Methods

## 3.2.1 Preparation of a model tablet

It was found that the mechanical properties of PlayDoh can be affected by the batch and color of PlayDoh, and humidity of the environment (Tardos et al., 2004). The dark green PlayDoh particles from the same batch were coated with a layer of MgSt. A mixture of approximately 30 glass beads (1 mm diameter) and 40 MgSt coated PlayDoh particles was compressed into a model cylindrical tablet (11.28 mm diameter) by a compaction simulator (Styl'One, Medelpharm, Beynost, France) at 120 MPa using a saw tooth profile with 40 ms loading and unloading without a hold at the peak load.

## 3.2.2 Micro computed tomography (Micro-CT)

Micro-CT is a non-destruction 3D imaging technique that employs X-rays to visualize the internal structures of a specimen, allowing us to examine the deformation of particles in a tablet after compression (Busignies et al., 2006). Micro-CT scanning of the glass bead – PlayDoh tablet was performed right after it was made on a micro-CT machine (XT H 225, Nikon Metrology Inc.,

Brighton, MI, USA), using the following parameters: 90 kV,  $110 \mu A$ , 708 ms of exposure, 720 projections, 4 frames per projection, and a voxel size of  $9.3 \mu m$ . The total image acquisition time was approximately 34 min for each run. 2D projections were subsequently processed to reconstruct a three-dimensional image of the sample by CT Pro (Nikon Metrology, Belgium). Visualization and analysis of the reconstructed 3D images was performed using VG Studio 3.4 (Volume Graphics GmbH, Germany).

## 3.2.3 Optical microscopy

Some of the PlayDoh particles and glass beads in the model tablet were manually separated and their images taken with a StereoZoom microscope (Leica MZ7.5, Feasterville, PA, USA).

# 3.2.4 Preparation of an ABA powder

Following a procedure described before (Cruz-Cabeza et al., 2019), the  $\beta$  form of p-aminobenzoic acid (ABA $\beta$ ) was obtained by suspending excess of the  $\alpha$  form (ABA $\alpha$ ) in distilled water at 4 °C under stirring for two weeks. The resulting powder was filtered and dried overnight in a 40 °C oven.

## 3.2.5 Powder X-ray diffractometry (PXRD)

A powder X-ray diffractometer (PANalytical X'pert pro, Westborough, MA, USA) with Cu K $\alpha$  radiation (1.54059 Å) was used to characterize the crystallographic properties of the ABA powders. Samples were scanned between 5° and 35° in 2 $\theta$  with a step size of 0.016° and a dwell time of 1 s/step. The X-ray tube voltage was set to 45 kV and amperage was set to 40 mA.

## 3.2.6 Blend preparation

All powders were passed a 355 µm sieve (mesh 460). Binary mixtures consisting of 40% of either ABA polymorph and 60% of an excipient (either MCC or DCPD) were placed in a 120 mL plastic bottle (Starplex, Cleveland, TN, USA) and mixed using a shaker mixer (Turbula T2F, Glen Mills Inc., Clifton, NJ, USA) for 15 min at 49 rpm. Then, 1% (w/w) MgSt was added to the mixture followed by further mixing for 1.5 min.

## 3.2.7 True density

The true density of water-containing powder, MCC, was determined by fitting compaction pressure (P) – tablet density  $(\rho)$  data to the Sun equation (Sun, 2005). True densities of all other samples were measured using a helium pycnometer (Quantachrome Instruments, Ultrapycnometer 1000e, Byonton Beach, FL, USA). An accurately weighed sample was placed into the sample cell, occupying approximately half to three-quarters of the cell volume. The measurement was concluded once the standard deviation of five successive measurements was less than 0.005% and the mean of the last five measurements was then taken as the sample's true density  $(\rho_t)$ . The  $\rho_t$  of mixtures was calculated from  $\rho_t$  and weight percentage of constituting components.

## 3.2.8 Tableting of ABA powders and their formulations

A compaction simulator (Styl'One, Medelpharm, Beynost, France) was used to prepare a series of tablets with approximately 200 mg of each powder at compaction pressures ranging from 25 to 350 MPa with a dwell time of 63 ms, simulating a Korsch XL100 press running at 31 rpm. Round (8 mm diameter) flat-faced punches were used for all compactions. Tablet dimensions were measured using a digital caliper to calculate tablet density. The tablets were broken diametrically using a texture analyzer (TA-XT2i, Texture Technologies Corp., Scarsdale, NY, USA) at a speed of 0.001 mm/s with a 5 g trigger force. Tablet tensile strength ( $\sigma$ ), was calculated using Eq. (1) from the maximum breaking force (F), tablet diameter (d), and tablet thickness (h), following a standard procedure (Fell and Newton, 1970).

$$\sigma = \frac{2F}{\pi dh} \tag{1}$$

Tablet porosity ( $\varepsilon$ ) was calculated from tablet envelope density ( $\rho$ ) and true density ( $\rho_t$ ) of powder using equation (2).

$$\varepsilon = 1 - \frac{\rho}{\rho_t} \tag{2}$$

Tabletability was characterized by a plot of tensile strength as a function of compaction pressure (P), while compressibility was characterized by a plot of tablet porosity against P. Compactibility was characterized by a plot of tensile strength as a function of tablet porosity.

193

194

195

196

197

190

191

192

# 3.2.9 In-die Heckel analysis

In-die Heckel analysis was conducted following a standard procedure (Vreeman and Sun, 2021), where the linear portion of the in-die tablet porosity,  $\varepsilon$ , vs. P plot was analyzed based on the Heckel equation (3), to obtain the mean yield pressure  $P_{\gamma}$  (Heckel, 1961a, 1961b).

$$-\ln(\varepsilon) = \frac{1}{P_y}P + A \tag{3}$$

199

200

201

202

203

204

205

206

207

208

209

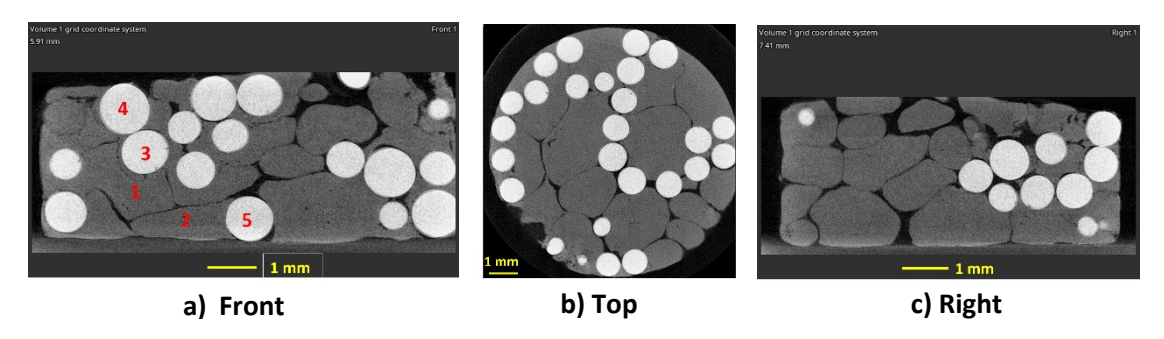
210

211

#### 4. Results and discussion

## 4.1 Deformation behavior of particles

Because of the distinct mechanical properties of soft PlayDoh and hard glass beads, the PlayDoh-glass tablet exhibited soft-soft, hard-hard, and soft-hard modes of contact, making it suitable for examining the proposed BA-dominating mechanism (Figure 1). In fact, the hardness of PlayDoh and glass likely bracket the range of hardness of typical pharmaceutical powders, i.e., hardness of excipients and APIs likely distributes between them. The different radiopacities of PlayDoh and glass allowed easy distinction between the two types of particles, facilitating the visualization of BA between particles (Figure 2). In the micro-CT images, the glass beads appeared white, the PlayDoh particles were grey, and air appeared black. Despite the uniform size of the glass beads, different cross-sections were captured on a given 2D plane, resulting in circular areas with different diameters equal to or smaller than 1 mm.



212

**Figure 2.** The micro-CT images (2D slices) of a PlayDoh-glass bead tablet along the planes of three principal directions a) front-x, b) top-z, c) right-y.

In the front cross section of the micro-CT images, three types of contacts can be identified, i.e., 1) PlayDoh-PlayDoh, 2) glass-glass, and 3) PlayDoh-glass (Figure 2a). The interfaces of type 1 contacts, i.e., those between adjacent soft PlayDoh particles (e.g., 1-2), were approximately flat, reflecting the similar compliance of adjacent particles during compression. Type 2 contacts were point-like (e.g., 3-4), as the applied compression was insufficient to cause permanent deformation of hard glass beads. The substantially larger BA formed at type 1 contacts compared to type 2 explains the superior tabletability of more plastic API solid forms (Figure 1a and 1b). Type 3 contacts (e.g., 1-3 and 2-5) involved the soft PlayDoh particles enveloping the hard glass beads. The interfaces of types 1 and 3 contacts are also depicted in the optical images of particles separated after compression in Figure 3. Thus, the BA follows the descending order of soft-hard > soft-soft >> hard-hard. This finding from a model tablet supports the hypothesis that a significantly larger BA is developed in the case of hard-soft contacts than in the case of soft-soft contacts during compaction.

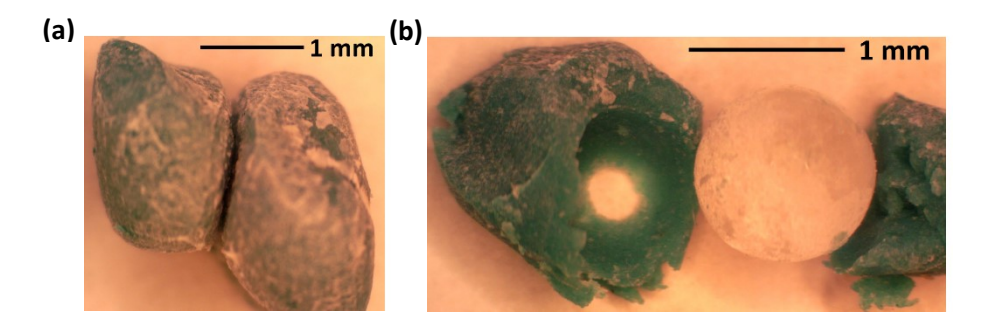


**Figure 3.** Optical microscopic images of contact areas between a) PlayDoh and PlayDoh particles (type 1), and b) PlayDoh and glass bead (type 3). The diameter of the glass bead is 1 mm.

## 4.2 Testing the hypothesis using the ABA polymorph system

The hypothesized BA-dominating mechanism predicts that tabletability flip only occurs when two API solid forms with a large difference in plasticity are each mixed with a soft excipient but not with a hard excipient. To test this hypothesis further, we studied an ABA polymorphic

system with MCC as the soft excipient and DCPD as the hard excipient. TFP was previously observed in a system of 20% (w/w) ABA polymorphs with 80% MCC (Wang et al., 2023). In this work, 40% ABA and 60% MCC were used. The plasticity of these materials follows the descending order of ABA $\alpha \ge$  MCC > ABA $\beta >>$  DCPD, as suggested by their in-die  $P_y$  values (Table 1).

**Table 1.** In-die  $P_{\nu}$  values of materials studied in this work.

Material	In-die $P_y$ (MPa)
MCC	55.7 (0.4) *
DCPD	681.4 (3.7) *
$ABA\alpha$	51.5 (1.8)
ΑΒΑβ	109.0 (6.4)

<sup>\*</sup>Vreeman and Sun, 2021

The identity of the two ABA polymorphs was confirmed by comparing their experimental PXRD patterns with those calculated from corresponding single crystal structures (Alleaume et al., 1966; Lai and Marsh, 1967), where closely matched peak positions were observed (Figure 4a). The different peak intensities observed in the  $2\theta$  range of 20 to 35 degrees in the experimental and calculated PXRD patterns of ABA $\alpha$  are attributed to the preferred orientation of crystals (Zhang et al., 2020).

The four materials investigated in this study exhibited distinct tabletability, with MCC demonstrating the best tabletability, while ABAβ failed to form intact tablets over the entire pressure range (Figure 4b). According to the tabletability classification based on the BA-BS interplay model (Sun, 2011), MCC falls into the Class I category (high BA and high BS), while DCPD belongs to the Class IV category (low BA, high BS). It was anticipated that the BA in DCPD tablets was substantially smaller than those in the other three materials due to its significantly lower plasticity (Table 1). However, the positive effect of its higher BS appeared to have more than compensated for the negative effect of the smaller BA, resulting in having higher tensile strengths than both ABA polymorphs when the compaction pressure was 100 MPa or higher (Figure 4b). Given that the BSs of the two ABA polymorphs are comparable due to the same

molecular structure (i.e., difference in surface energies is small), the superior tabletability of ABA $\alpha$  compared to ABA $\beta$  is attributed to the formation of a larger BA. This follows from the higher plasticity of ABA $\alpha$ , as indicated by its lower  $P_y$  value (Table 1). In contrast, ABA $\beta$  failed to form intact tablets under all investigated compaction pressures, most likely due to negligible plastic deformation during compaction, and much lower BS compared to DCPD.

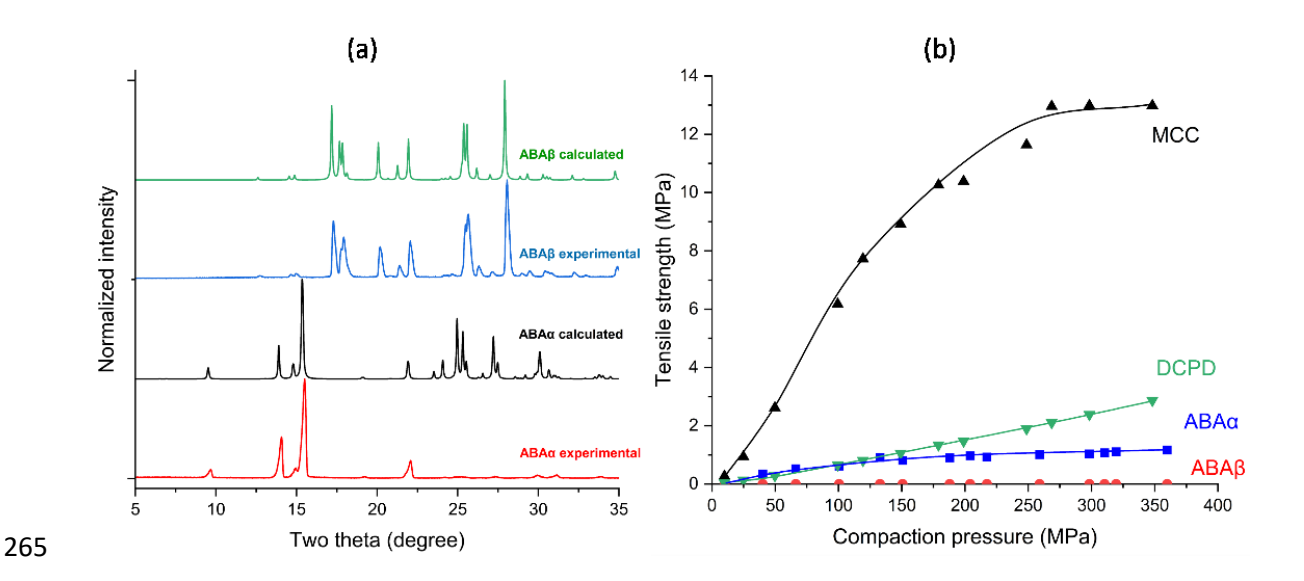


**Figure 4.** a) PXRD patterns of two ABA polymorphs; b) tabletability plots of materials studied in this work.

When MCC was used, the ABA $\alpha$ -MCC mixture fell into the soft-soft mixture category, while the ABA $\beta$ -MCC mixture was classified as a hard-soft mixture based on their in-die  $P_y$  values (Table 1). Consequently, the TFP was predicted based on the BA-dominating mechanism. Indeed, the tabletability of the ABA $\beta$ -MCC mixture was found to be higher than that of the ABA $\alpha$ -MCC mixture, with the difference in tensile strength becoming increasingly larger with rising compaction pressure (Figure 5a). This observed trend aligns with findings from previous studies (Paul et al., 2020; Wang et al., 2023).

The BA-dominating mechanism also predicts that the TFP would not occur when mixing with a hard excipient. To test this prediction, we used DCPD, known for its significantly lower plasticity compared to both polymorphs of ABA (Table 1), as the expedient. The experimental results confirmed the prediction, as the tabletability of the ABAβ-DCPD mixture was consistently

lower than that of the ABA $\alpha$ -DCPD mixture across the entire range of compaction pressures studied (Figure 5b).

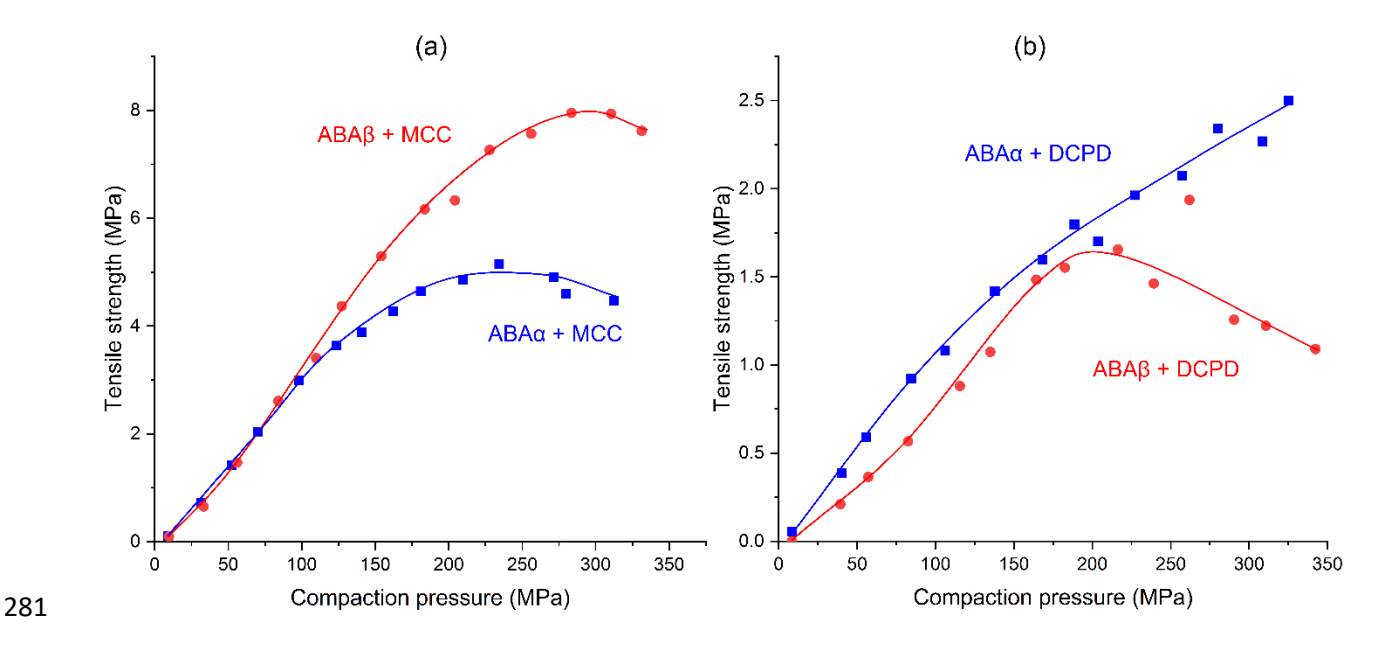


Figure 5. Tabletability plots of ABA polymorphs with a) MCC and b) DCPD.

# 4.3 Features of TFP explained by the BA-dominating mechanism

The occurrence and extent of the TFP were observed to depend on the compaction pressure and the difference in plasticity between the two materials in the mixture, as highlighted in a previous study (Wang et al., 2023). These effects can now be elucidated by the BA-dominating mechanism.

In all the studied systems that exhibit TFP, a notable observation is that tabletability flip tends to be more prominent at higher compaction pressures. This phenomenon can be explained by considering the deformation behavior of different mixtures under pressures outlined in the BA dominating mechanism. At low pressures, a soft-hard mixture undergoes less extensive plastic deformation than a soft-soft mixture because the percolating matrix of hard particles resists consolidation of the powder bed more. Meanwhile, the extent of a soft particle conforming to the shape of a neighboring hard particle is low, resulting in a smaller BA in the soft-hard mixture tablet than the soft-soft mixture tablet and TFP may not occur. As the pressure increases, the tensile strength of the soft-soft mixture increases slowly because BA, which has largely developed in the low-pressure process, only increases slowly, In a tablet consisting of soft and hard particles, on the

other hand, the soft particles continue to undergo appreciable amount of plastic deformation with increasing pressure, resulting in a larger BA and higher tensile strength. Above a critical pressure, the overall BA in a soft-hard tablet surpasses that in a soft-soft tablet, resulting in the occurrence of TFP. For the same reason, the difference in tensile strength between the two mixtures becomes more pronounced at higher pressures.

The extent of the TFP also depends on the difference in plasticity between the API powders. For example, only marginal TFP occurred in systems of similar plasticity with MCC, e.g., crystalline acetaminophen ( $P_y = 80.8 \pm 2.4$ MPa) and its amorphous solid dispersion in Copovidone ( $P_y = 89.5 \pm 2.7$  MPa) (Wang et al., 2023). In contrast, pronounced TFP was observed in systems of APIs with a large difference in plasticity with MCC, e.g., Ibuprofen ( $P_y = 22.1 \pm 2.5$  MPa) and L-alanine ( $P_y = 231.0 \pm 2.8$  MPa) (Wang et al., 2023). This dependence can be explained by the BA-dominating mechanism. When the plasticity between two API powders is comparable, the BA would be similar when they are each mixed with the same excipient, resulting in marginal, if any, TFP. However, when two API powders with a significant difference in plasticity are each mixed with a soft excipient, the BA-dominating mechanism leads to a large difference in BA and pronounced TFP (Figure 1).

## 4.4 Caution in the application of compressibility and compactibility plots

When explaining the tabletability of different powders using the BA-BS interplay model, it is necessary to access reliable BA and BS of the powders. Because of the difficulty with quantifying BA in a tablet, compressibility is commonly used as an indirect assessment of BA between tablets, where a lower porosity under the same pressure is assumed to correspond to a larger BA in the compact if particle size and shape are not significantly different. Compactibility, on the other hand, is commonly used to characterize BS, where the tensile strength at zero porosity,  $\sigma_0$ , is used to compare the BS of two powders assuming the BAs are the same at zero porosity. In fact, compressibility and compactibility plots combined with a tabletability plot, which are also known as "CTC" analysis, are widely used to investigate the compaction properties of materials (Bowles et al., 2018; Katz and Buckner, 2017; Khomane et al., 2013; Patel et al., 2006; Persson et al., 2022; Tye et al., 2005; Yadav et al., 2018; Yu et al., 2020). However, it should be pointed out that, for tablets exhibiting identical porosity, their BA is influenced by particle size, particle morphology, and the shape of the contact planes between particles. Consequently, caution must be

exercised when using compressibility to assess BA, i.e., the assumption of the same BA at zero porosity is likely inaccurate. Similarly, since the true BS is conceptually the total attractive forces per unit BA, the BS derived from the compactibility profile is also affected by the factors that influence BA. Hence,  $\sigma_0$  can only represent an "apparent BS" instead of the true BS (Shi and Sun, 2024). We take the opportunity here, using ABA systems exhibiting TFP, to emphasize the point that blindly applying compressibility and compactibility to quantify BA and BS, respectively, without addressing their limitations may be misleading.

When the two ABA polymorphs were each mixed with MCC, the compressibility plots of the two mixtures were nearly identical, i.e., comparable porosity at a given pressure (Figure 6a). Meanwhile, ABA $\beta$ -MCC exhibited better compactibility compared to ABA $\alpha$ -MCC, i.e., higher tensile strength at zero porosity (Figure 6b). Without considering the shape of the contact interface, one may conclude that the overall BA between the two mixtures is comparable and the BS in ABA $\beta$ -MCC is higher than that in ABA $\alpha$ -MCC. This analysis would have suggested a "BS-dominant mechanism" of the TFP, which contradicts the BA-dominating mechanism established earlier in this work for this system (Figures 2 and 3). This example highlights the need for caution when assessing BA and BS using compressibility and compactibility profiles, respectively.

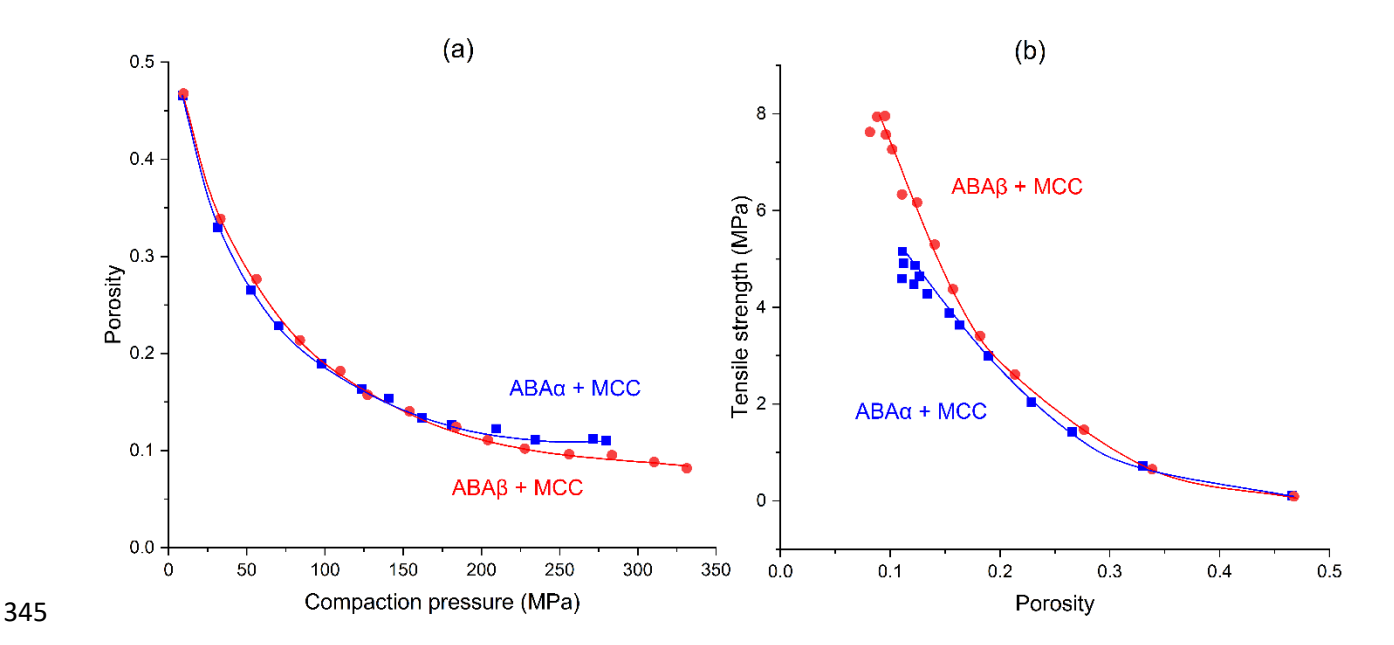


Figure 6. a) Compressibility and b) compactibility plots of ABA polymorphs with MCC.

## 4.5 Benefits and limitations of the BA dominating mechanism

The BA-dominating mechanism can not only elucidate the TFP but also offer invaluable insights into designing efficient and reliable tablet formulations. According to this mechanism, the addition of a plastic excipient into a poorly compressible hard API can significantly enhance tabletability of the formulation because of improved BA. Similarly, the blending of a soft API with a hard excipient into a "soft-hard" mixture may also maintain the tabletability in the formulation. Thus, this mechanism can offer a theoretical basis for the empirical rule of thumb of maintaining a plasticity – brittleness balance when designing a tablet formulation. However, the TFP is affected by numerous factors. The effectiveness of improving tabletability through establishing soft-hard contact also depends on the spatial distribution of each constituent and their particle properties, such as size and shape. In addition to plasticity, other mechanical properties, such as elasticity, viscoelasticity, and brittleness, also affect the BA during compression. Hence, a systematic investigation of the impact of these influencing factors is required to accurately predict tabletability and, hence, TFP.

We wish to point out that the BA-dominating mechanism is applicable only when the plasticity of the softer API is comparable to the excipient. When the plasticity of both API powders is significantly lower than that of the excipient, the occurrence of TFP is likely due to a BS-dominant mechanism. In that case, the BA is comparable in both mixtures since the softer excipient conforms to the shape of the particles of both API forms in a similar way, even if one API is much harder than the other. Consequently, the mixture with the harder API form can exhibit a higher tabletability if it has a higher BS. However, this BS-dominant mechanism for TFP also requires a systematic investigation into the potential influencing factors to confirm. Finally, it should be pointed out that the BA-BS interplay model is so far qualitative in nature, which provides a conceptual framework for understanding various tableting phenomena. However, applying it for quantitative predictions of tabletability is extremely difficult, if not impossible.

#### 5. Conclusions

The proposed BA-dominating mechanism provides a very plausible explanation for the TFP in systems where an excipient with plasticity similar to that of the softer API solid form is used to prepare powder mixtures. The mechanism suggests that, in such cases, the soft excipient particles conform to the shape of the hard API particles but form an approximately flat bonding

interface with soft API particles, resulting in a larger BA in the "soft-hard" mixture than the "soft-soft" mixture. The validity of this mechanism has been substantiated through visual demonstrations of plastic deformation of particles in model mixtures comprising both soft and hard particles, utilizing micro-CT and optical microscopy. Experimental verification of the predicted occurrence of TFP with a soft excipient and its predicted absence with a hard excipient for two ABA polymorphs further supports this mechanism. The mechanism is also consistent with the observed influence of the compaction pressure and the difference in plasticity of the API solid forms on the TFP. Additionally, this study highlights a potential pitfall in assessing the BA and BS using, respectively, the compressibility and compactibility profiles. By considering the possibility of a BA-dominating mechanism, one may gain a deeper understanding of the complex interplay between mechanical properties, particulate properties, and compaction conditions in tablet formulation design.

390

378

379

380

381

382

383

384

385

386

387

388

389

#### ACKNOWLEDGMENT

CCS thanks the National Science Foundation for support through the Industry University Collaborative Research Center (IUCRC) grant IIP-2137264, Center for Integrated Materials Science and Engineering for Pharmaceutical Products (CIMSEPP).

#### References

- Alleaume, M., Salas-Cimingo, G., Decap, J., 1966. Comptes Rendus Seances de l'Academie des Sciences. Ser, C 262, 416–417.
- Bowles, B.J., Dziemidowicz, K., Lopez, F.L., Orlu, M., Tuleu, C., Edwards, A.J., Ernest, T.B., 2018. Co-Processed Excipients for Dispersible Tablets—Part 1: Manufacturability. AAPS PharmSciTech 19, 2598–2609. https://doi.org/10.1208/s12249-018-1090-4
- Busignies, V., Leclerc, B., Porion, P., Evesque, P., Couarraze, G., Tchoreloff, P., 2006. Quantitative measurements of localized density variations in cylindrical tablets using X-ray microtomography. Eur. J. Pharm. Biopharm. 64, 38–50. https://doi.org/10.1016/j.ejpb.2006.02.007
- Chang, S.-Y., Sun, C.C., 2017. Superior Plasticity and Tabletability of Theophylline Monohydrate. Mol. Pharm. 14, 2047–2055. https://doi.org/10.1021/acs.molpharmaceut.7b00124
- Chen, H., Zhang, J., Qiao, Q., Hu, E., Wei, Y., Pang, Z., Gao, Y., Qian, S., Zhang, J., Heng, W., 2022. A novel soluble lornoxicam-sodium chelate monohydrate with improved plasticity and tabletability. Int. J. Pharm. 624, 122060. https://doi.org/10.1016/j.ijpharm.2022.122060

- Cocks, A.C.F., Sinka, I.C., 2007. Constitutive modelling of powder compaction I. Theoretical concepts. Mech. Mater. 39, 392–403. https://doi.org/10.1016/j.mechmat.2006.09.003
- Cruz-Cabeza, A.J., Davey, R.J., Oswald, I.D.H., Ward, M.R., Sugden, I.J., 2019. Polymorphism in p-aminobenzoic acid. CrystEngComm 21, 2034–2042. https://doi.org/10.1039/C8CE01890A
- Fell, J.T., Newton, J.M., 1970. Determination of Tablet Strength by the Diametral-Compression Test. J. Pharm. Sci. 59, 688–691. https://doi.org/10.1002/jps.2600590523
- Galen, S., Zavaliangos, A., 2005. Strength anisotropy in cold compacted ductile and brittle powders. Acta Mater. 53, 4801–4815. https://doi.org/10.1016/j.actamat.2005.06.023
- Heckel, R.W., 1961a. An analysis of powder compaction phenomena. Trans Met. Soc AIME 221, 1001–1008.
- Heckel, R.W., 1961b. Density–Pressure Relationships in Powder Compaction. Trans Met. Soc AIME 221, 671–675.
- Hu, S., Mishra, M.K., Sun, C.C., 2019. Twistable Pharmaceutical Crystal Exhibiting Exceptional Plasticity and Tabletability. Chem. Mater. 31, 3818–3822. https://doi.org/10.1021/acs.chemmater.9b00441
- Katz, J.M., Buckner, I.S., 2017. Full Out-of-Die Compressibility and Compactibility Profiles From Two Tablets. J. Pharm. Sci. 106, 843–849. https://doi.org/10.1016/j.xphs.2016.11.005
- Khomane, K.S., More, P.K., Raghavendra, G., Bansal, A.K., 2013. Molecular Understanding of the Compaction Behavior of Indomethacin Polymorphs. Mol. Pharm. 10, 631–639. https://doi.org/10.1021/mp300390m
- Lai, T.F., Marsh, R.E., 1967. The crystal structure of p-aminobenzoic acid. Acta Crystallogr. 22, 885–893. https://doi.org/10.1107/S0365110X67001720
- Li, F., Pan, J., Sinka, C., 2009. Contact laws between solid particles. J. Mech. Phys. Solids 57, 1194–1208. https://doi.org/10.1016/j.jmps.2009.04.012
- Mckenna, A., Mccafferty, D.F., 1982. Effect of particle size on the compaction mechanism and tensile strength of tablets. J. Pharm. Pharmacol. 34, 347–351. https://doi.org/10.1111/j.2042-7158.1982.tb04727.x
- Nyol, S., Gupta, M.M., 2013. IMMEDIATE DRUG RELEASE DOSAGE FORM: A REVIEW. J. Drug Deliv. Ther. 3. https://doi.org/10.22270/jddt.v3i2.457
- Patel, S., Kaushal, A., Bansal, A., 2006. Compression Physics in the Formulation Development of Tablets. Crit. Rev. Ther. Drug Carrier Syst. 23, 1–65. https://doi.org/10.1615/CritRevTherDrugCarrierSyst.v23.i1.10
- Paul, S., Tajarobi, P., Boissier, C., Sun, C.C., 2019. Tableting performance of various mannitol and lactose grades assessed by compaction simulation and chemometrical analysis. Int. J. Pharm. 566, 24–31. https://doi.org/10.1016/j.ijpharm.2019.05.030
- Paul, S., Wang, C., Sun, C.C., 2020. Tabletability Flip Role of Bonding Area and Bonding Strength Interplay. J. Pharm. Sci. 109, 3569–3573. https://doi.org/10.1016/j.xphs.2020.09.005
- Persson, A.-S., Pazesh, S., Alderborn, G., 2022. Tabletability and compactibility of α-lactose monohydrate powders of different particle size. I. Experimental comparison. Pharm. Dev. Technol. 27, 319–330. https://doi.org/10.1080/10837450.2022.2051550
- Rudnic, M.J.K., Edward M., 2002. Tablet Dosage Forms, in: Modern Pharmaceutics, Fourth Edition Revised and Expanded. CRC Press.

- Shi, L., Sun, C.C., 2024. Understanding the roles of compaction pressure and crystal hardness on powder tabletability through bonding area bonding strength interplay. Int. J. Pharm.
- Sinka, I.C., Motazedian, F., Cocks, A.C.F., Pitt, K.G., 2009. The effect of processing parameters on pharmaceutical tablet properties. Powder Technol., Special Issue: 3rd International Workshop on Granulation: Granulation across the Length Scales 189, 276–284. https://doi.org/10.1016/j.powtec.2008.04.020
- Sun, C. C., 2005. True Density of Microcrystalline Cellulose. J. Pharm. Sci. 94, 2132–2134. https://doi.org/10.1002/jps.20459
- Sun, C.C., Grant, D.J.W., 2001. Influence of Crystal Structure on the Tableting Properties of Sulfamerazine Polymorphs. Pharm. Res. 18, 274–280. https://doi.org/10.1023/A:1011038526805
- Sun, C.C., 2011. Decoding Powder Tabletability: Roles of Particle Adhesion and Plasticity. J. Adhes. Sci. Technol. 25, 483–499. https://doi.org/10.1163/016942410X525678
- Sun, C.C., 2009. Materials science tetrahedron--a useful tool for pharmaceutical research and development. J. Pharm. Sci. 98, 1671–1687. https://doi.org/10.1002/jps.21552
- Tardos, G.I., Hapgood, K.P., Ipadeola, O.O., Michaels, J.N., 2004. Stress measurements in high-shear granulators using calibrated "test" particles: application to scale-up. Powder Technol., 1st International Workshop on Granulation (Granulation across the length scales: linking microscopic experiments and models to real process operation) 140, 217–227. https://doi.org/10.1016/j.powtec.2004.01.015
- Tye, C.K., Sun, C.C., Amidon, G.E., 2005. Evaluation of the effects of tableting speed on the relationships between compaction pressure, tablet tensile strength, and tablet solid fraction. J. Pharm. Sci. 94, 465–472. https://doi.org/10.1002/jps.20262
- Ubhe, T.S., Gedam, P., 2020. A Brief Overview on Tablet and It's Types. J. Adv. Pharmacol. 1, 21–31.
- Vreeman, G., Sun, C.C., 2021. Mean yield pressure from the in-die Heckel analysis is a reliable plasticity parameter. Int. J. Pharm. X 3, 100094. https://doi.org/10.1016/j.ijpx.2021.100094
- Wang, Z., Wang, C., Bahl, D., Sun, C.C., 2023. The ubiquity of the tabletability flip phenomenon. Int. J. Pharm. 643, 123262. https://doi.org/10.1016/j.ijpharm.2023.123262
- Yadav, J.P.A., Bansal, A.K., Jain, S., 2018. Molecular Understanding and Implication of Structural Integrity in the Deformation Behavior of Binary Drug–Drug Eutectic Systems. Mol. Pharm. 15, 1917–1927. https://doi.org/10.1021/acs.molpharmaceut.8b00077
- Yu, Y., Zhao, L., Lin, X., Wang, Y., Feng, Y., 2020. A model to simultaneously evaluate the compressibility and compactibility of a powder based on the compression ratio. Int. J. Pharm. 577, 119023. https://doi.org/10.1016/j.ijpharm.2020.119023
- Zavaliangos, A., Laptev, A., 2000. The densification of powder mixtures containing soft and hard components under static and cyclic pressure. Acta Mater. 48, 2565–2570. https://doi.org/10.1016/S1359-6454(00)00066-5
- Zhang, L., Gonçalves, A., Jaroniec, M., 2020. Identification of preferentially exposed crystal facets by X-ray diffraction. RSC Adv. 10, 5585–5589. https://doi.org/10.1039/D0RA00769B